Supporting Information

Potentiating light-harvest tactics through A-D-A structure: repolarization tumor associated macrophage through phototherapy

Pai Liu*[a, f], Xinyue Zhao[b], Jiayu Cao[c], Mengyan Tian[a], Yaning Li[a], Chunyan Ma[d], Tianyue Yang[a], Yi Liu *[c, e, f]

[a] *State Key Laboratory of Separation Membranes and Membrane Processes, School of Materials Science and Engineering, Tiangong University, Tianjin 300387, P. R. China.*

[b] *School of Chemical Engineering and Technology, Tiangong University, Tianjin 300387, P. R. China.*

[c] *School of Chemistry, Tiangong University, Tianjin 300387, P. R. China.*

[d] *School of Life Science, Tiangong University, Tianjin 300387, P. R. China.*

[e] *School of Chemical and Environmental Engineering, Wuhan Polytechnic University, Wuhan 430023, P. R. China.*

[f] *Cangzhou Institute of Tiangong University, Cangzhou 061000, P. R. China.*

* Corresponding authors.

E-mail addresses: yiliuchem@whu.edu.cn, Liupai@tiangong.edu.cn

Materials used in experiments

All materials were used directly without further purification.

4-bromo-N,N-di-p-tolylaniline, 5-formyl-2-thiopheneboronic acid, Pd(dppf)Cl_2, K_2CO_3, para-toluidine, 1-bromo-4-iodobenzene, [$Pd_2(dba)_3$], dppf, sodium tert-butoxide and malononitrile were purchased from Tianjin Chemart Chemical Reagent Co. Ltd. Dichloromethane, trichloromethane, petroleum ether, toluene, methanol were purchased from Tianjin Chemart Chemical Reagent Co. Ltd. 3-(4,5-Dimethyl-2-thiazolyl)-2,5-diphenyl-2H-tetrazolium bromide (MTT), dichlorodihydrofluorescein diacetate (DCFH-DA), phosphate buffered saline (PBS), rose bengal (RB), 9,10-anthracenediyl-bis(methylene)-dimalonic acid (ABDA), hydroxyphenyl fluorescein (HPF) and dihydrorhodamine 123 (DHR123) were purchased from Tianjin Chemart Chemical Reagent Co. Ltd.5,5-dimethyl-1-pyrroline-N-oxide (DMPO) and 2,2,6,6-tetramethyl-4-piperidone hydrochloride (TEMP) were purchased from Beijing InnoChem Science & Technology Co. Ltd. Dulbecco's modifies eagle medium (DMEM) and fetal bovine serum (FBS) were purchased from Wuhan Servicebio Biotechnology Co. Ltd. Lyso-Tracker Green, Annexin V-FITC/PI Apoptosis Detection Kit and Calcein-AM/PI Double Stain Kit were purchased from Shanghai Beyotime Biotechnology Co. Ltd. Recombinant Mouse IL-4 (C-6His**)** was purchased from Beijing Solarbio Technology Co. Ltd. The FITC anti-Mouse CD206 Antibody, PE anti-Mouse CD206 Antibody, CD206 Antibody, CD86 Antibody, APC anti-Mouse CD86 Antibody and PE anti-Mouse CD86 Antibody were purchased from Affinity Biosciences Co. Ltd.

Instruments used in experiments

The absorption spectra was recorded by UV-6100 Double Beam Spectrophotometer (Shanghai Mapada Instruments Co. Ltd.). Photoluminescence (PL) spectra was recorded by Gangdong F-320 fluorescence spectrophotometer (Tianjin Gangdong Sci.&Tech. Co. Ltd.). ^{1}H-NMR and ^{13}C-NMR spectra were recorded by Bruker Avance 400MHz spectrometer using dimethyl sulfoxide-d6 (DMSO-d_6) as

solvents. ESI-mass Spectrometry were measured on Thermo TSQ from Beijing Ernst Testing Technology Co. Ltd. ESR anaiysis was conducted on Bruker Elexsys 500 X-band EPR spectrometer. Size distribution was analyzed on a dynamic light scattering (DLS) using Nexis GD-2060 from Malvern. Photothermal experiments were implemented by using a Nd:YAG Laser surgery equipment (TY532-150) and FLIR E8-XT camera. The cell viability was detected by MTT assay kit, and the absorbance of each sample was measured at 490 nm using a VICTOR Nivo Multimode Reader. Cell imaging was performed on an Olympus FV3000 confocal laser scanning microscope (CLSM). Agilent NovoCyte flow cytometry was used to test the relevant parameters of the cells. *In vivo* imaging of 4T1 tumor-bearing mice were achieved through Tanon ABL X5 PRO.

Synthesis

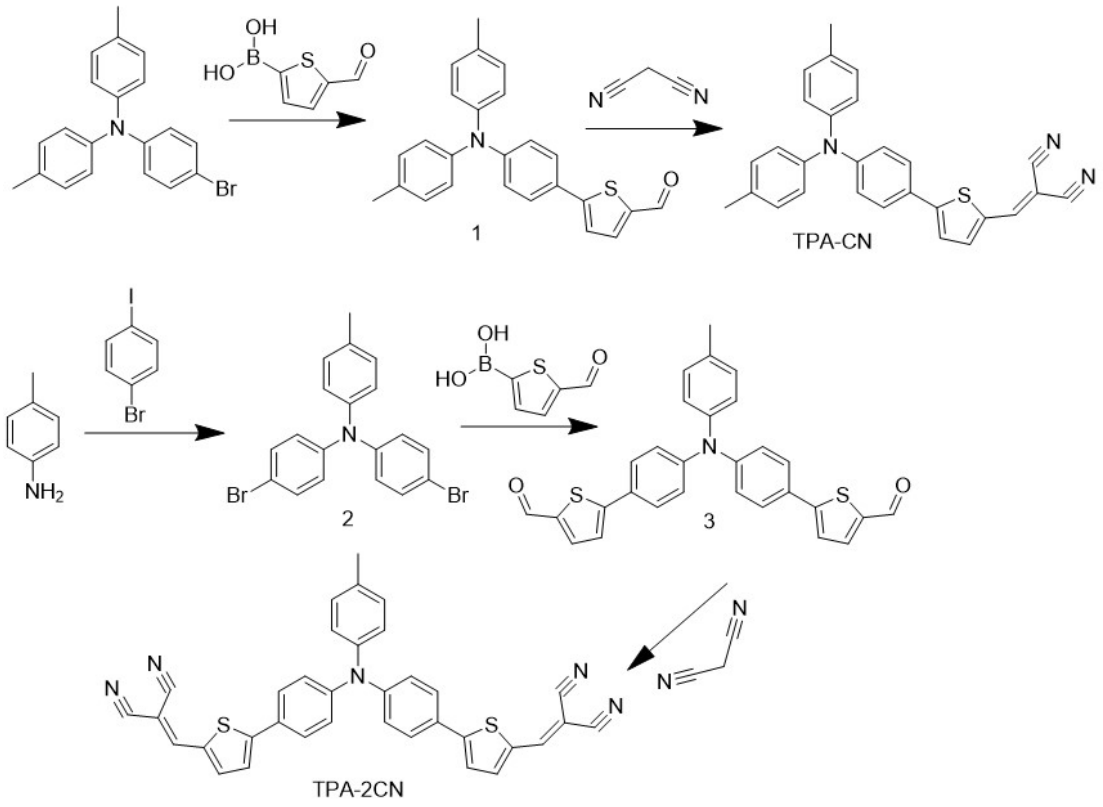

Scheme S1. The synthetic routes of TPA-CN and TPA-2CN

Synthesis of compound 1: A solution of 4-bromo-N, N-di-p-tolylaniline (352mg, 1 mmol), 5-formyl-2-thiopheneboronic acid (156 mg, 1.3 mmol), Pd(dppf)Cl_2 (73.2 mg, 0.1 mmol) and K_2CO_3 (690 mg, 5 mmol) were refluxed under nitrogen in dry methanol and toluene mixture (1:1, v/v) at 75℃ for 24 h. After cooling to room temperature, the solvent were removed and the residue were extracted with dichloromethane (DCM) and water. The crude product was purified by a silica gel column chromatography using petroleum ether/DCM (1:1, v/v) as eluent to give a golden powder of compound 1 (310.8 mg, 81% yield). ^{1}H NMR (400 MHz, DMSO-d_6) δ=9.86 (s, 1H), 8.00 (d, 1H), 7.65 (d, 2H), 7.58 (d, 1H), 7.17 (d, 4H), 7.00 (d, 4H), 6.88 (d, 2H), 2.29 (s, 6H).

Synthesis of TPA-CN: Two drops of triethylamine were added to a mixture of compound 1 (38.4 mg, 0.1 mmol) and malononitrile (7.9 mg, 0.12 mmol) in $CHCl_3$ (5 mL). The reaction mixture were refluxed for 12 h. After completion of the reaction as monitored by thin layer chromatography (TLC), the reaction mixture were cooled and evaporated to afford a residue which were then purified by silica-gel column chromatography using DCM and petroleum ether mixtures as the eluent to obtain a red-brown solid TPA-CN (26.3 mg, 61% yield). ^{1}H NMR (400 MHz, DMSO-d_6) δ=7.91 (d, 1H), 7.82–7.52 (m, 4H), 7.18 (d, 4H), 7.02 (d, 4H), 6.88 (d, 2H), 2.30 (s, 6H). ^{13}C NMR (101 MHz, DMSO-d_6) δ=152.84, 150.06, 144.05, 143.42, 134.35, 133.20, 130.82, 128.18, 126.04 ,124.49, 124.06, 120.30, 115.42, 114.66, 73.35, 20.96. HRMS (ESI, positive mode, m/z): calcd: 432.15, found: 432.15.

Synthesis of compound 2: Para-toluidine (270 mg, 2.52 mmol), 1-bromo-4-iodobenzene (1485 mg, 5.25 mmol), [$Pd_2(dba)_3$] (25 mg, 0.025 mmol), dppf (40 mg, 0.075 mmol) and sodium tert-butoxide (675 mg, 7.0 mmol) were refluxed under nitrogen in dry toluene at 115℃ for 36 h. After cooling to room temperature, the solvent were removed and the residue were extracted with DCM and water. The crude product were purified by column chromatography on petroleum ether to give compound 2 as a white crystalline solid (705.2 mg, 67%). ^{1}H NMR (400 MHz, DMSO-d_6) δ=7.49–7.35 (m, 4H), 7.17 (d, 2H), 7.03–6.93 (m, 2H), 6.94–6.86 (m, 4H), 2.28 (s, 3H).

Synthesis of compound 3: Compound 2 (417 mg, 1 mmol), 5-formyl-2-thiopheneboronic acid (468 mg, 3 mmol), Pd(dppf)Cl_2 (73.2 mg, 0.1 mmol) and Cs_2CO_3

(1629 mg, 5 mmol) were refluxed under nitrogen in dry methanol and toluene mixture (1:3, v/v) at 75°C for 24 h. After cooling to room temperature, the solvent were removed and the residue were extracted with DCM and water. The crude product were purified by a silica gel column chromatography using petroleum ether/DCM (1:2 v/v) as eluent to give a golden powder of compound 3 (129 mg, 27% yield). ^{1}H NMR (400 MHz, DMSO-d_6) δ=9.91 (d, 2H), 8.03 (d, 2H), 7.79–7.70 (m, 4H), 7.65 (d, 2H), 7.23 (d, 2H), 7.07 (d, 6H), 2.32 (s, 3H).

Synthesis of TPA-2CN: Two drops of triethylamine were added to a mixture of compound 3 (48 mg, 0.1 mmol) and malononitrile (19.8 mg, 0.3 mmol) in DCM (5 mL). The reaction were refluxed for 2 h. Then petroleum ether were added in precipitation to obtain red and black solid precipitation, which were purified by column chromatography with DCM to obtain blood-red solid TPA-2CN (37.5 mg, 65% yield). ^{1}H NMR (400 MHz, DMSO-d_6) δ=8.00 (d, 2H), 7.91–7.60 (ddd, 8H), 7.30 (d, 2H), 7.21–7.05 (dd, 6H), 2.39 (s, 3H). ^{13}C NMR (101 MHz, DMSO-d_6) δ=152.98, 148.67, 143.31, 135.42, 133.83, 132.09, 131.14, 129.14, 128.33, 126.59), 125.23, 123.51, 115.28, 114.53, 74.20, 21.03. HRMS (ESI, positive mode, m/z): calcd: 575.12, found: 575.12.

Total ROS generation testing in solution using DCFH-DA

75 μL 2',7'-Dichlorodihydrofluorescein diacetate (DCFH-DA, 40 μM) as an indicator and 15 μL TPA-CN/TPA-2CN (1 mM) were added into 2910 μL PBS. Control group was prepared by adding 15 μL RB (1 mM) and 75 μL DCFH-DA into 2910 μL PBS. After that, the obtained solutions were exposed to irradiation (10 mW cm^{-2}) for different time, the PL intensities at 532 nm were recorded under excitation at 488 nm.

$^1O_2$ testing in solution using ABDA

30 μL 9,10-Anthracenediyl-bis(methylene)-dimalonic acid (ABDA, 1 mM) as an indicator and 15 μL TPA-CN/TPA-2CN (1 mM) were added into 2955 μL water upon irradiation (10 mW cm^{-2}) for different time, the absorption spectra of ABDA was measured. The relative absorption (A/A_0) at 378 nm versus irradiation time was then

recorded. Besides, ABDA with RB was tested under the same experimental procedures as the control group, ABDA as a singlet oxygen indicator.

•O_2^- testing in solution using DHR123

100 μL Dihydrorhodamine 123 (DHR123, 150 μM) as an indicator and 15 μL TPA-CN/TPA-2CN (1 mM) were added into 2885 μL PBS. Control group was prepared by adding 100 μL DHR123 and 15 μL DMSO into 2885 μL PBS. After that, the obtained solutions were exposed to irradiation (10 mW cm^{-2}) for different time, the PL intensities at 530 nm were recorded under excitation at 488 nm.

•OH testing in solution using HPF

200 μL Hydroxyphenyl fluorescein (HPF, 2 μM) as an indicator and 2 μL TPA-CN/TPA-2CN (1 mM) were added into 798 μL PBS. Control group were prepared by adding 200 μL HPF and 2 μL DMSO into 798 μL PBS. After that, the obtained solutions were exposed to irradiation (10 mW cm^{-2}) for different time, the PL intensities at 525 nm were recorded under excitation at 488 nm.

ESR analysis

ESR analysis was conducted to confirm the generation of •O_2^- and •OH with DMPO as a radical trap. MeOH (1.96 mL, 9 M), DMPO (20 μL) and TPA-CN (or TPA-2CN) (20 μL, 1 mM) were mixed. Then, the spectra were obtained after the corresponding solutions were exposed to irradiation (10 mW cm^{-2}) for 5 min. For $^1O_2$, deionized water (1.96 mL), TEMP (20 μL, 10 M) and TPA-CN (or TPA-2CN) (20 μL, 1 mM) were mixed. Then, the spectra were obtained after exposed to irradiation (10 mW cm^{-2}) for 5 min.

Computational methods

The density functional theory (DFT) method was used to optimize geometries of TPA-CN and TPA-2CN at the levels of b3lyp/6-311g* within Gaussian 09 Package. The excited energies and spin-orbit coupling (SOCs) between singlet and triplet states were calculated by the time-dependent density functional theory (TD-DFT) method at the level of M06-2X/6-311g* within ORCA 4.0 Package.

Photothermal properties tests

The solution of TPA-CN, TPA-2CN (10 μM) and DMSO were irradiated by 532 nm laser (0.5 W cm^{-2}) for 5 min. The temperature changes were monitored by FLIR E8-XT camera. Different concentrations of TPA-2CN were prepared (0 μM, 10 μM, 20 μM, 50 μM and 100 μM) and irradiated by 0.5 W cm^{-2} with 532 nm laser for 5 min. The temperature changes were monitored during irradiation. The photothermal conversion efficiency of TPA-2CN was determined referring to previously reported publications.[1] The solution of TPA-2CN (50 μM) was exposed to 532 nm laser irradiation at 0.5 W cm^{-2} for 5 min when its temperature reached a plateau. At this time point, the laser was shut off. Then the solution was cooled down to room temperature. The temperature of the solution was recorded at an interval of 60 s during this process.

Cell viability test

The 4T1 cells were seeded on 96-well plates at a density of 1×10^4 cells/well for 24 h incubation. Subsequently, the medium was replaced with the fresh medium containing different concentrations of TPA-CN and TPA-2CN. After further incubation for 4 h, The cells were irradiated for different time. Meanwhile, TPA-CN and TPA-2CN incubated cells without irradiation were also conducted for the dark cytotoxicity study. After further incubation for 4 h, the media was removed and washed with PBS for three times. Cells were then incubated with fresh MTT solution (5 mg/mL in PBS). After 4 h, 100 μL of DMSO was added into each well to dissolve the formazan, Finally, the absorbance of the products was measured at a wavelength of 490 nm by a microplate reader. The results were expressed as the viable percentage of cells after different

treatments relative to the control cells without any treatment. The relative cell viability was calculated according to the following formula:

$$\text{Cell viability (\%)} = [(OD_{sample} - OD_{background})/(OD_{control} - OD_{background})] \times 100\%$$

CLSM analysis of intracellular ROS

4T1 cells were seeded in confocal dishes at a density of 1×10^5 cells and incubated for 24 h. Then the medium was replaced with TPA-2CN (20 μM) and cultured continuously for 2 h under dark. Then, the cells were thoroughly washed with PBS, incubated with DCFH-DA as ROS probe for 30 min, irradiated (10 mW cm^{-2}) for 5 min, and the intracellular ROS production was detected by CLSM after treatment.

Flow cytometry analysis of intracellular ROS

4T1 cells were seeded in confocal dishes at a density of 1×10^5 cells and incubated for 24 h. Then the medium was replaced by TPA-2CN (20 μM), and incubated continuously 2 h in dark, incubated with DCFH-DA as ROS probe for 30 min, irradiated (10 mW cm^{-2}) for 5 min, and the intracellular ROS production was detected by flow cytometry after treatment.

CLSM analysis of apoptosis and necrosis

4T1 cells were seeded in confocal dishes at a density of 1×10^5 cells and incubated for 24 h. The cells were then incubated with TPA-2CN (20 μM) for 2 h in fresh medium. Irradiated (10 mW cm^{-2}) for 5 min, the cells were cultured for another 4 h and then stained with calcein acetoxymethyl ester (Calcein AM) and propidium iodide (PI) for 30 min. Subsequently, the cells were imaged by CLSM.

Flow cytometry analysis of apoptosis and necrosis

4T1 cells were seeded in confocal dishes at a density of 1×10^5 cells and incubated for 24 h. Then the medium was replaced by TPA-2CN (20 μM), and incubated continuously about 4 h in dark condition. Next, the cells were washed thoroughly with PBS and irradiated (10 mW cm^{-2}) for 5 min, after the treatment, the cells were further cultured for 4 h. The experiment was repeated using a laser (532 nm, 0.5 W cm^{-2}). The cells apoptosis and necrosis analysis were determined by Annexin V-FITC Apoptosis Detection Kit and flow cytometry.

Immunofluorescence assay

Bone marrow derived macrophages were seeded into 6-well culture plates at a density of 10^5 per well and incubated overnight at 37°C, followed by treatment with IL-4 (10 ng/mL) for 48 h to induce the M2-polarization. Then, TPA-2CN (10 μM) was added to the wells for 4 h followed by irradiation (10 mW cm^{-2}, 5 min). After treatment for 24 h, the macrophages in each group were collected, fixed in 4% paraformaldehyde for 30 min and stained with CD86 Antibody and CD206 Antibody at 4°C for 12 h. Then cells were washed three times with 1× PBS buffer and incubated with FITC secondary antibody and TRITC secondary antibody for 1 h at room temperature. The cell nuclei was stained with DAPI for 2 min at room temperature. Thereafter, the cells were washed with PBS and analyzed by CLSM.

TPA-2CN polarized M2 towards M1 phenotype *in vitro*

Bone marrow derived macrophages were seeded into 6-well culture plates at a density of 10^5 per well and incubated overnight at 37°C, followed by treatment with IL-4 (10 ng/mL) for 48 h to induce the M2-polarization. Then, TPA-2CN (10 μM) was added to the wells for 4 h followed by irradiation (10 mW cm^{-2}, 5 min). After treatment for 24 h, the macrophages in each group were collected, washed with flow cytometry staining buffer, and stained with PE anti-Mouse CD86 antibody and FITC Anti-Mouse CD206 Antibody at 4°C for 30 min. Thereafter, the cells were washed with PBS and analyzed by a flow cytometer.

Animals

Animals: BALB/c (female, 4 weeks) mice were purchased from the Tianjin YiShengYuan Bio-Technology Co.LTD.

Feeding conditions: all the animals were submitted to controlled temperature conditions (23 ~ 26℃), humidity (50 ~ 60%) and light (12 h light/12 h dark).

In vivo biodistribution and tumor-targeting capacity

BALB/c mice (female, 4 weeks) bearing 4T1 tumors (≈200 mm^3) were administered intravenous injection with 100 μM (100 μL) of TPA-2CN. At different time intervals (0, 2, 4, 8 and 12 h), the mice were imaged using an *in vivo* fluorescence imaging system.

In vivo therapeutic studies

BALB/c mice (female, 4 weeks, 12 in total) bearing 4T1 tumors (≈200 mm^3) were randomly divided into four groups (3 in each group), Control group, administration with PBS (100 μL) alone; Irradiation group, PBS administration (100 μL) followed by irradiation; TPA-2CN group, administration with TPA-2CN(100 μM, 100 μL); TPA-2CN+ Irradiation group, administration with TPA-2CN (100 μM, 100 μL) and followed by irradiation. For the photothermal therapy studies, 12 h after the intravenous injection, mice were irradiated with 532 nm laser (0.5 W cm^{-2}) for 5 min. The temperatures of the tumor area were measured with a photothermal camera (Fotric 285#L21) every min for 5 min. For the photodynamic therapy studies, 12 h after the intravenous injection, the mice were exposed to a light irradiated (10 mW cm^{-2}) for 5 min. During the treatment period, the tumor volume of all mice was measured every day using a vernier caliper. Then, the greatest longitudinal diameter (length) and the greatest transverse diameter (width) were used to calculate the tumor volume. Tumor volume V = length × $width^2$ /2. After treatment, tumors in all groups were weighed. At the end of tumor growth inhibition study, the tumor tissues of every group were digested into single-cell

suspensions. The cells were collected and dispersed in 1 mL of PBS after red blood cell lysis. The tumor-associated macrophages were stained with PE anti-Mouse CD206, APC anti-Mouse CD86, and then the cells were analyzed by flow cytometry. For histological analysis, the hematoxylin-eosin (H&E) staining and TdT-mediated dUTP Nick-End Labeling (TUNEL) staining of tumor slices and normal organs (heart, liver, spleen, lung, and kidneys) was carried out. Meanwhile, the fresh blood samples were collected for serum biochemistry text and blood routine.

In vivo biosafety assay

The hemocompatibility of TPA-CN and TPA-2CN at different concentrations was determined by the hemolysis method, and PBS and sterile water were used as the negative control group and the positive control group, respectively. Erythrocyte Centrifugation: blood was taken from the orbital vein of 4T1 mice and subjected to centrifugation (2000 rpm, 10 min, 4°C) and the supernatant was discarded. Preparation of erythrocyte suspension: A erythrocyte suspension was prepared by washing the erythrocytes three times with saline and resuspending the erythrocytes with saline. Control and experimental groups: Add appropriate amount of material to an equal volume of cell suspension. Equal volumes of saline were used as negative control and equal volumes of distilled water as positive control (both 1.25 mL), respectively. Constant temperature incubation: After gentle vortex mixing, the samples were incubated at 37°C for 3 h at a constant temperature. At the end of the incubation, the samples were centrifuged (2000 rpm, 10 min, 4°C) and the supernatant was discarded. 200 μL of the supernatant from the control and experimental groups were added to a 96-well plate and the absorbance at 450 nm was measured using an enzyme marker.

Hemolytic ratio (%) = $[(A_{sample} - A_{negative\ control})/(A_{positive\ control} - A_{negative\ control})] \times 100\%$

Statistical analysis

Statistical Analysis: Results were presented as mean ± SD. Significance was calculated using Least-Significant Difference with IBM SPSS Statistics: $*p < 0.05$, **

$p < 0.01$, *** $p < 0.001$ and **** $p < 0.0001$. The P-value < 0.05 was considered statistically significant.

Compounds characterization by NMR and HRMS

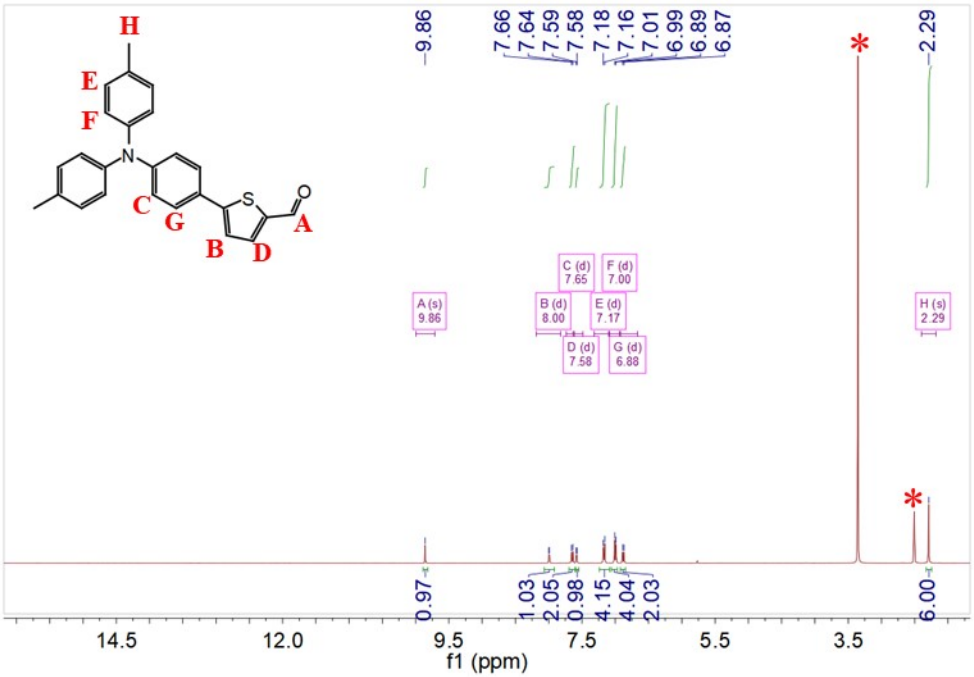

Figure S1. ^{1}H NMR spectra of compound **1** in DMSO-d_6.

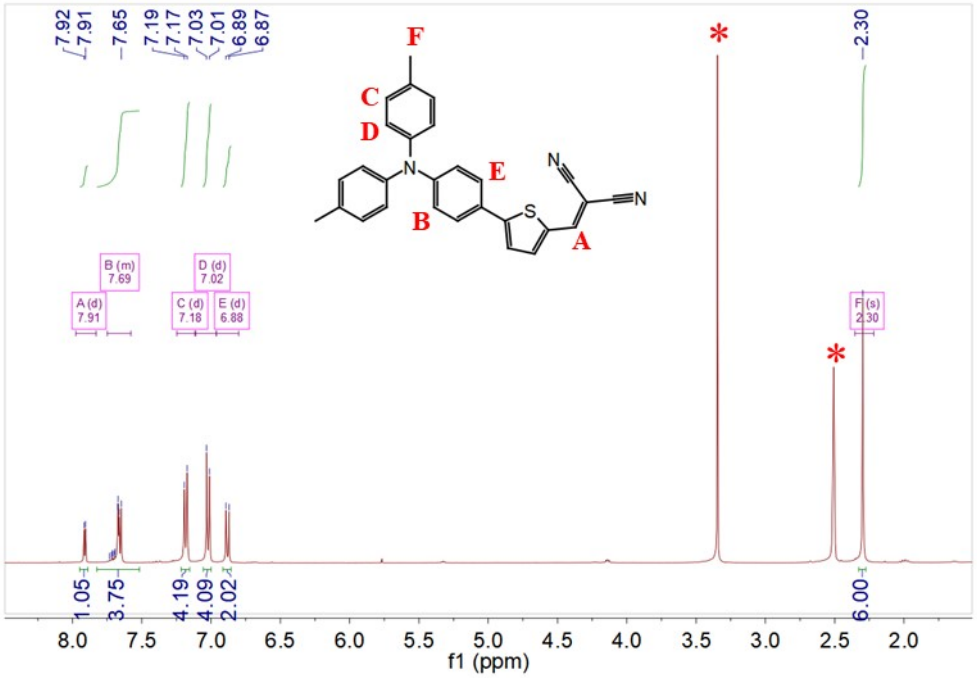

Figure S2. ^{1}H NMR spectra of TPA-CN in DMSO- d_6.

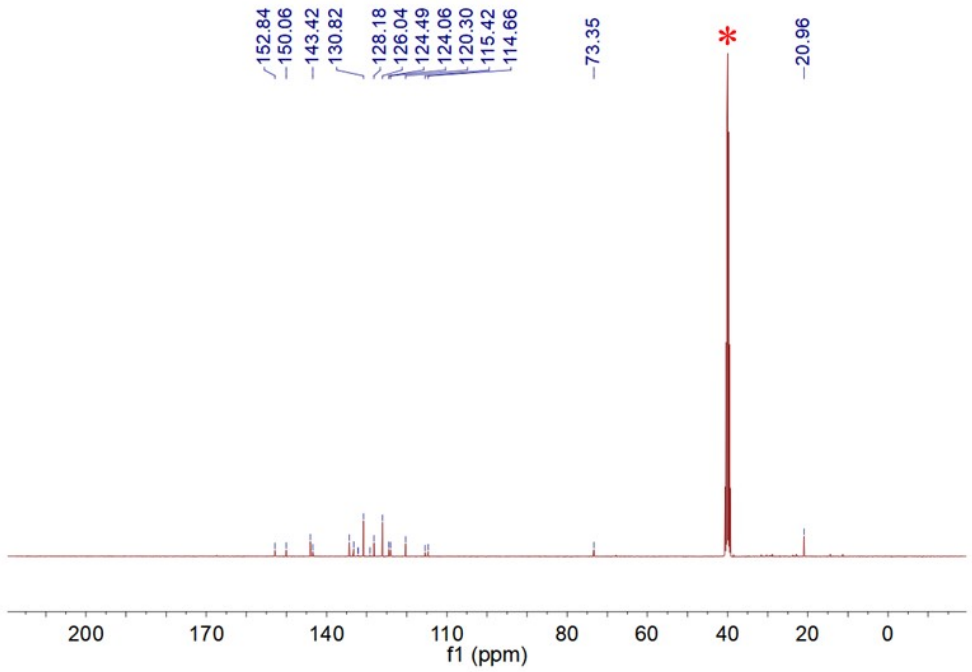

Figure S3. ^{13}C NMR spectra of TPA-CN in DMSO- d_6.

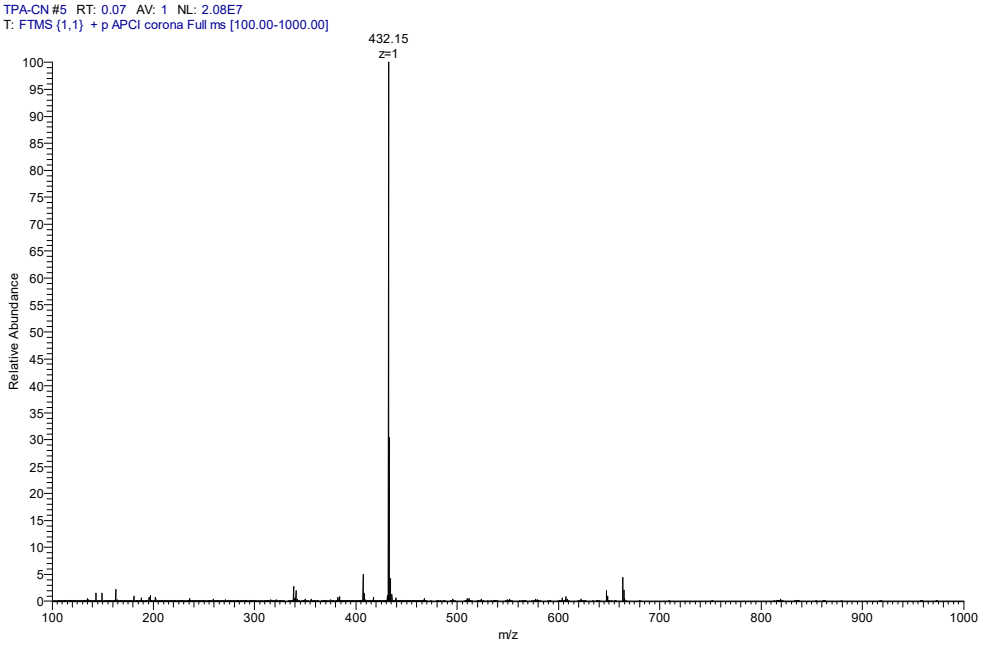

Figure S4. MS spectrum of TPA-CN.

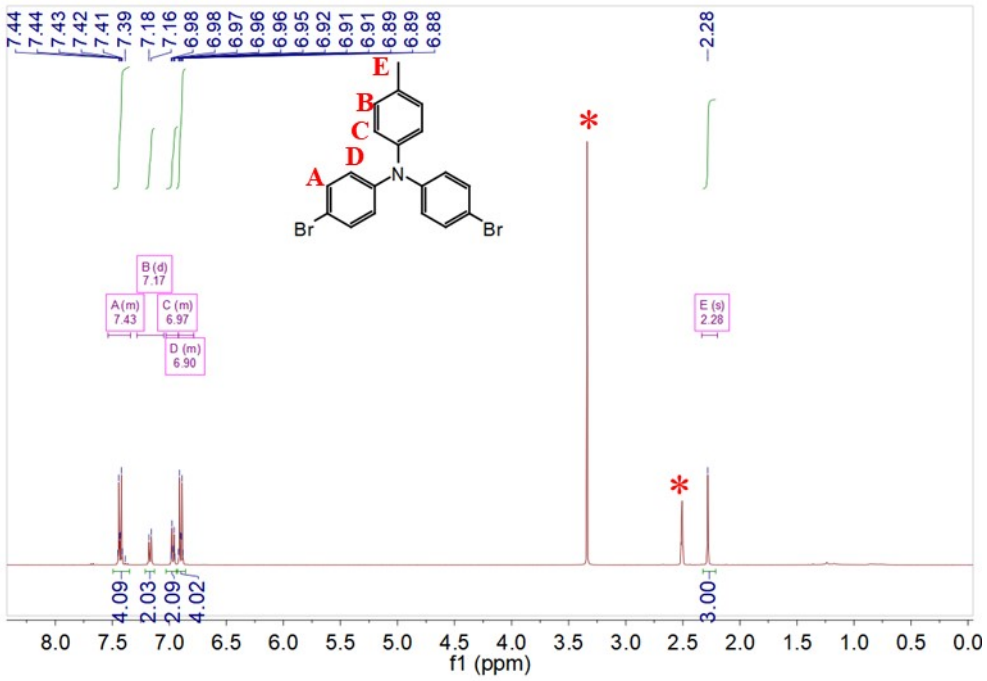

Figure S5. [1]H NMR spectra of compound **2** in DMSO- d_6.

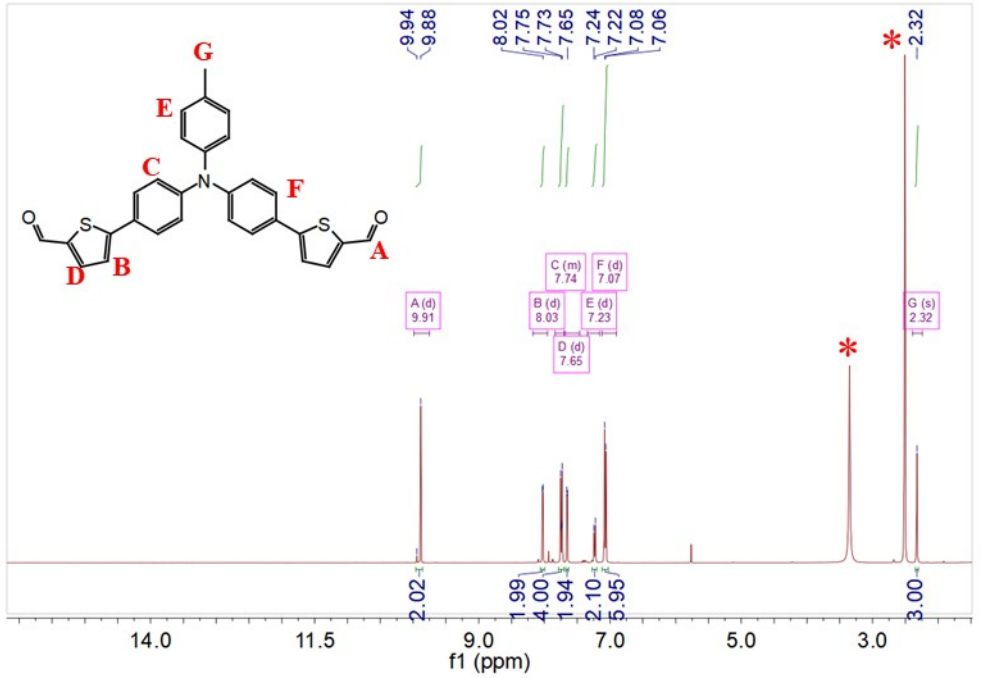

Figure S6. [1]H NMR spectra of compound **3** in DMSO- d_6.

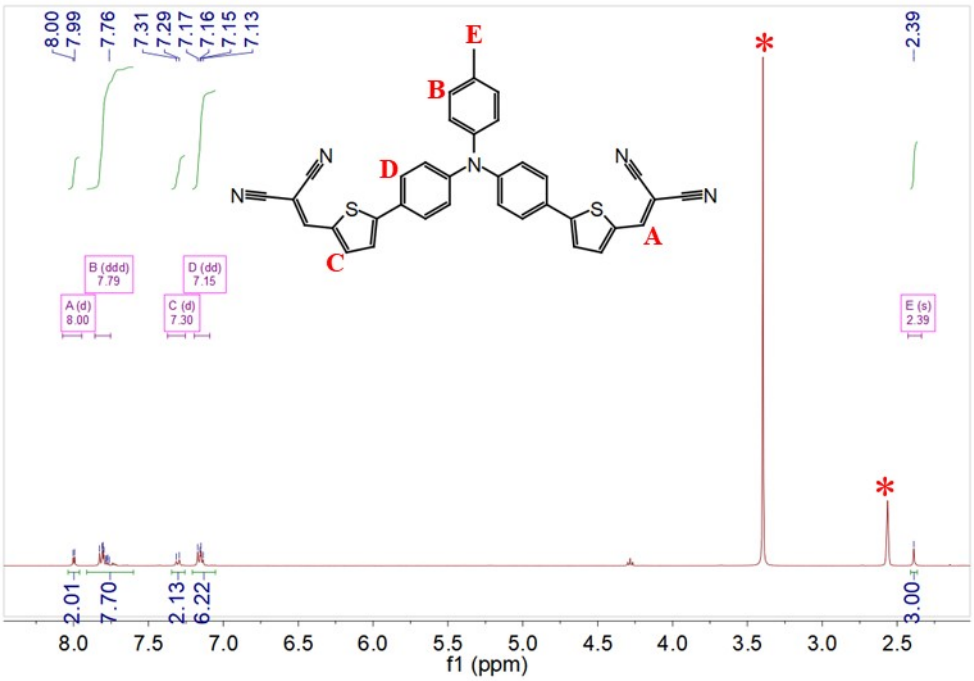

Figure S7. [1]H NMR spectra of TPA-2CN in DMSO- d_6.

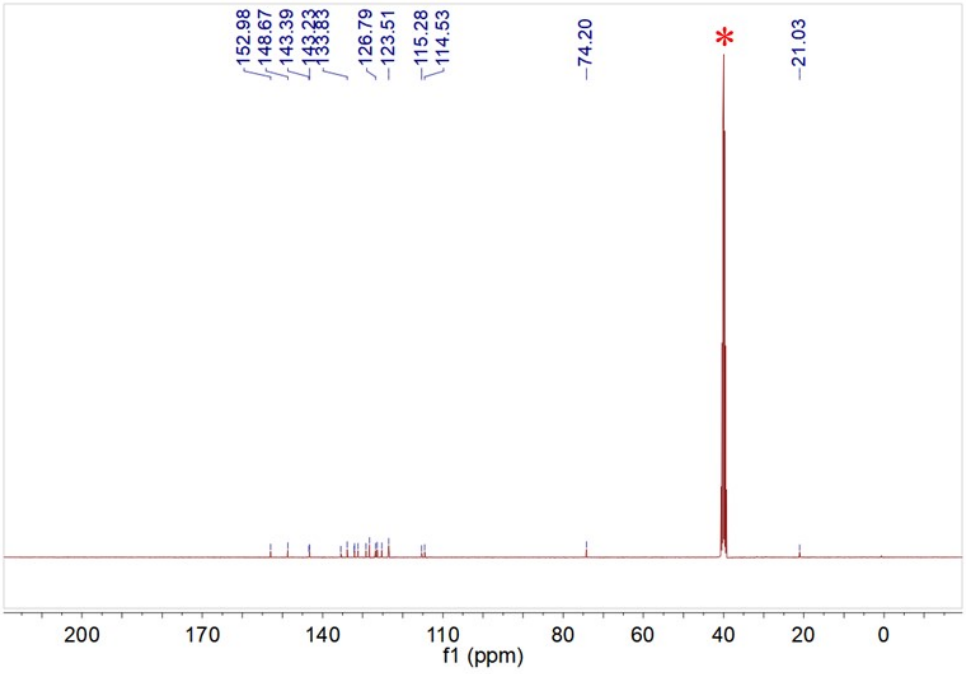

Figure S8. [13]C NMR spectra of TPA-2CN in DMSO- d_6.

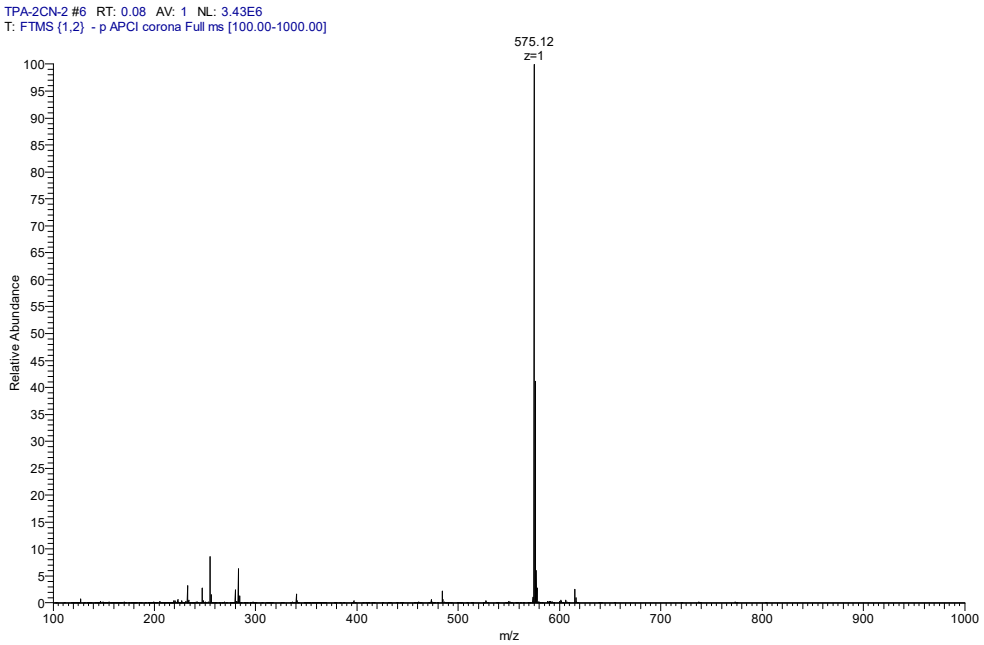

Figure S9. MS spectrum of TPA-2CN.

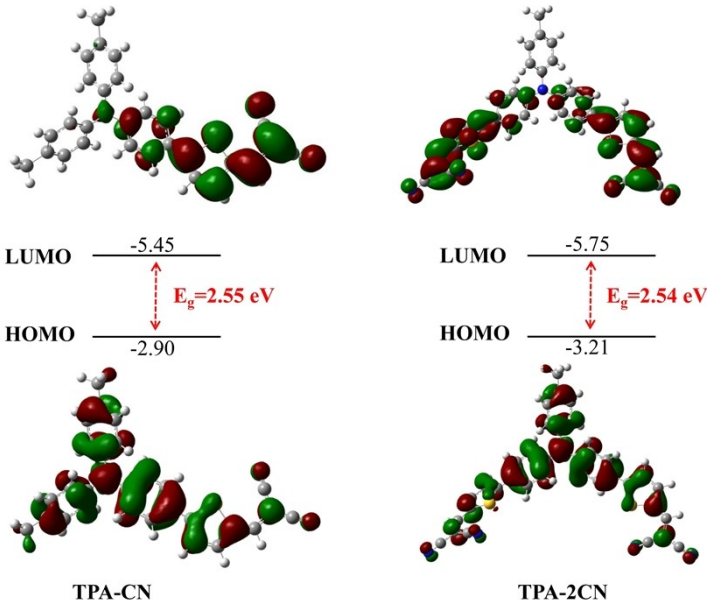

Figure S10. Frontier molecular orbitals and energies (eV) from DFT calculations of TPA-CN and TPA-2CN**.**

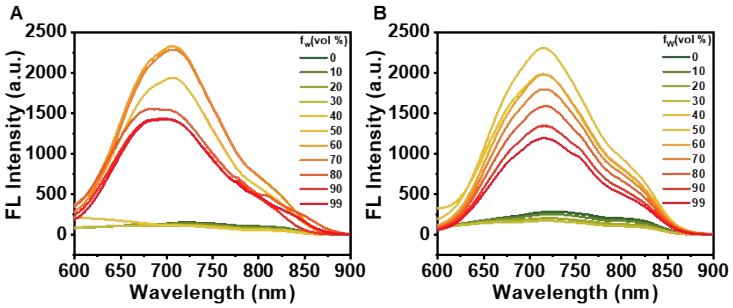

Figure S11. (A) PL spectra of TPA-CN (10 μM) in DMSO/water mixtures with different water fractions (f_w), λ_{ex}: 507 nm. (B) PL spectra of TPA-2CN (10 μM) in DMSO/water mixtures with different water fractions (f_w), λ_{ex}: 519 nm.

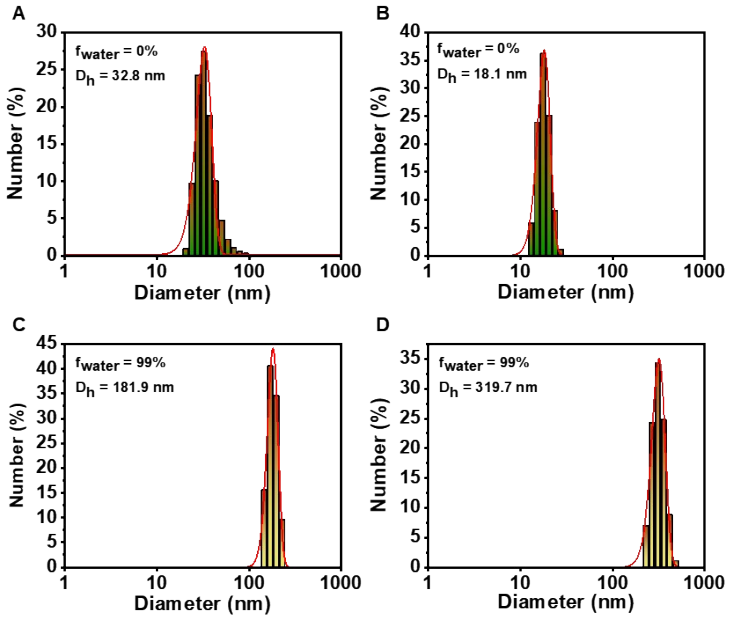

Figure S12. (A) and (C) Particle size distributions of TPA-CN aggregates in THF/water mixture with 0% or 99% water fraction. (B) and (D) Particle size distributions of TPA-2CN aggregates in DMSO/water mixture with 0% or 99% water fraction.

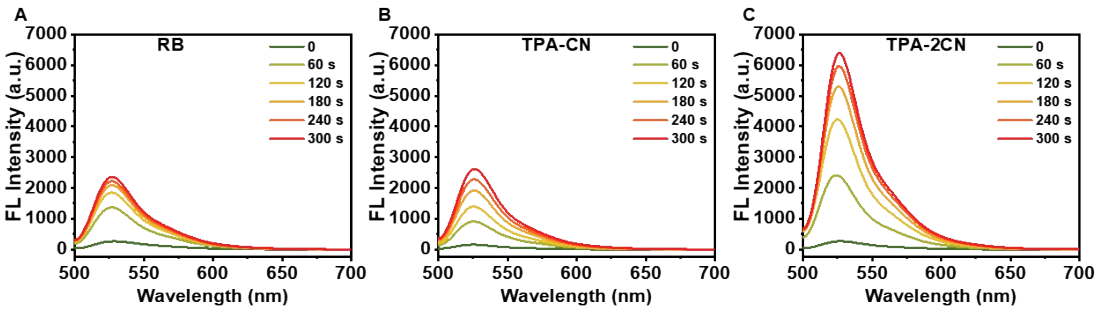

Figure S13. Fluorescence intensity of DCFH-DA for total ROS detection. (A) RB, (B) TPA-CN and (C) TPA-2CN (5 μM) with increasing irradiation time (10 mW cm^{-2}).

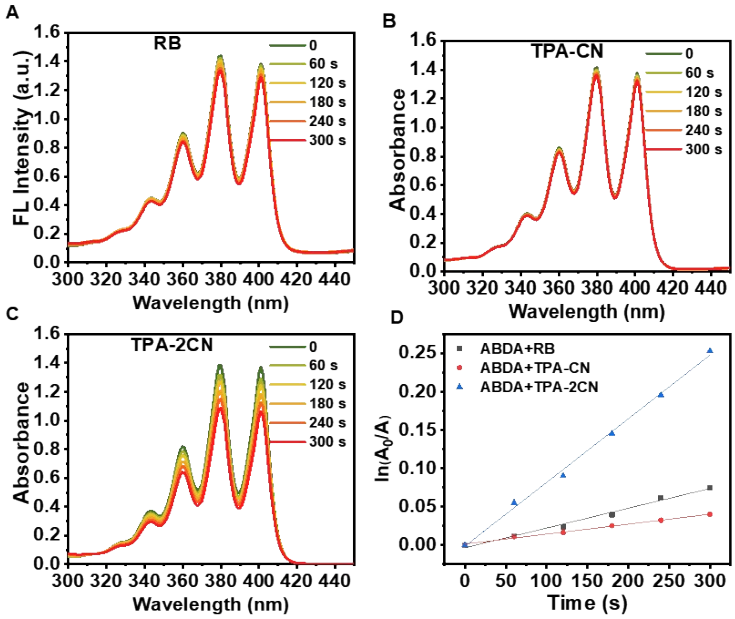

Figure S14. Absorption spectra of ABDA (used as a $^1O_2$ probe) observed in DMSO solution under different irradiation time in the presence of (A) RB, (B) TPA-CN, and (C) TPA-2CN in DMSO solution (10 mW cm^{-2}). (D) $^1O_2$ generation with the decomposition of ABDA (10 μM) for RB, TPA-CN and TPA-2CN (5 μM) under irradiation (10 mW cm^{-2}). A_0 represented the absorbance of ABDA before irradiation.

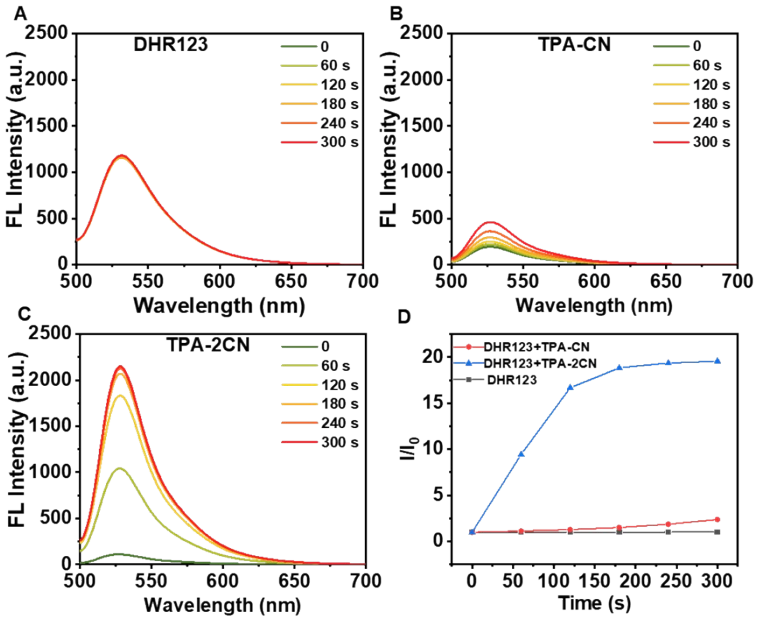

Figure S15. Fluorescence intensity changes of DHR123 for $\bullet O_2^-$ detection. (A) DHR123 only, (B) TPA-CN and (C) TPA-2CN (5 μM) with increasing irradiation time (10 mW cm^{-2}). (D) Plot of the relative emission intensity (I/I_0) of a DHR123 (5 μM) solution containing TPA-CN and TPA-2CN (5 μM) upon irradiation (10 mW cm^{-2}).

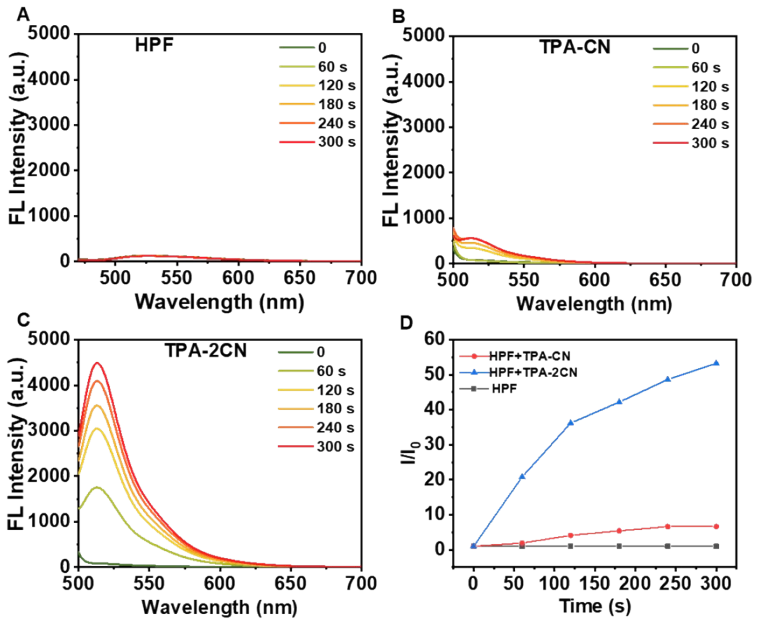

Figure S16. Fluorescence intensity changes of HPF for •OH detection. (A) HPF only, (B) TPA-CN and (C) TPA-2CN (5 μM) with increasing irradiation time (10 mW cm^{-2}). (D) Plot of the relative emission intensity (I/I_0) of a HPF (2 μM) solution containing TPA-CN and TPA-2CN (5 μM) upon irradiation (10 mW cm^{-2}).

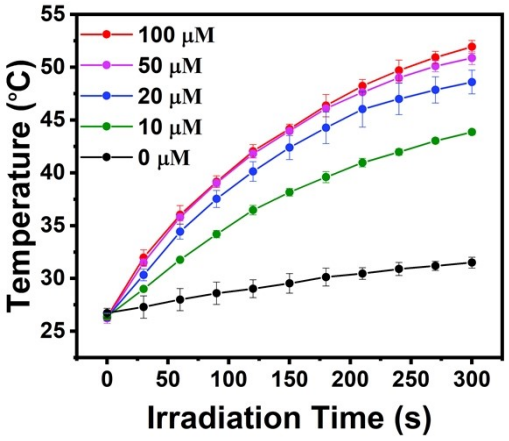

Figure S17. Photothermal property of TPA-2CN at different concentrations (0-100 μM) under 532 nm laser irradiation (0.5 W cm^{-2}).

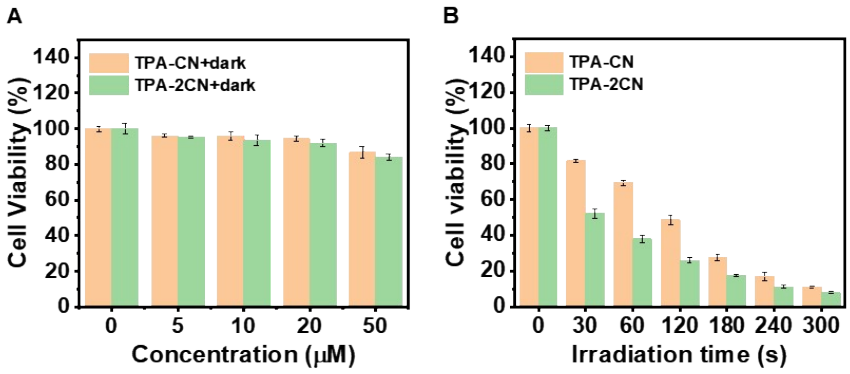

Figure S18. (A) Viabilities of 4T1 cells treated with different concentrations of TPA-CN and TPA-2CN (0-50 μM) in the absence of irradiation. (B) Cell survival rate under different irradation time (TPA-CN and TPA-2CN, 20 μM).

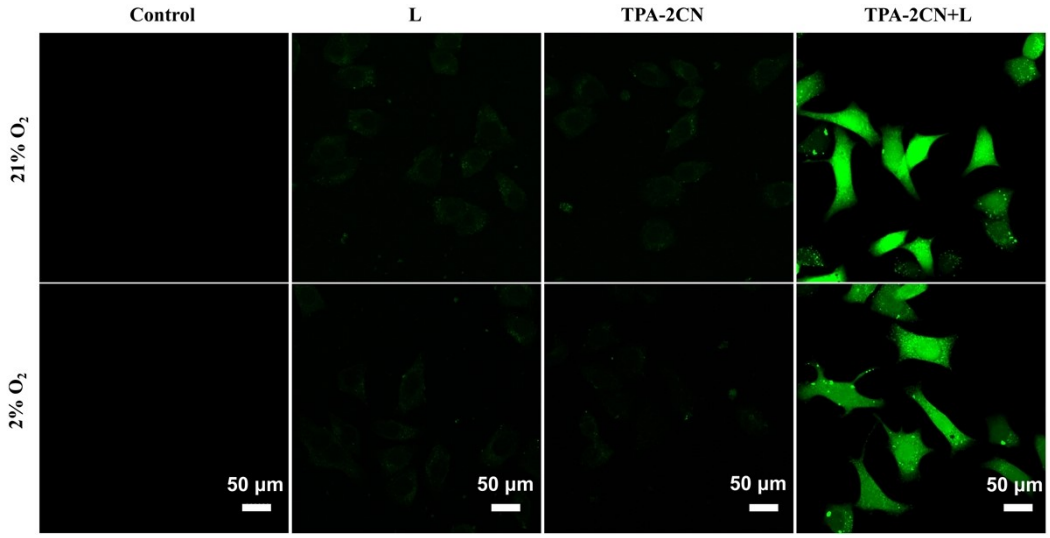

Figure S19. Intracellular ROS levels of 4T1 cells after different experimental treatments.

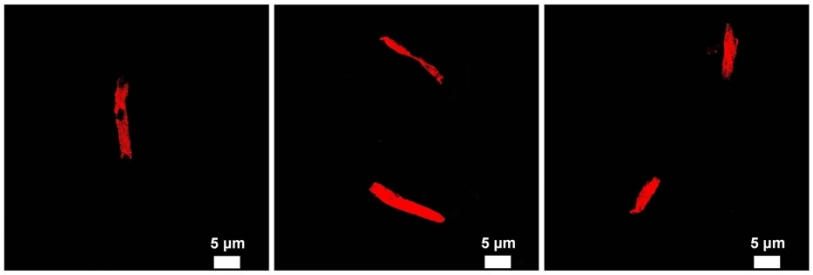

Figure S20. CLSM imaging of TPA-2CN (20 μM) in DMEM.

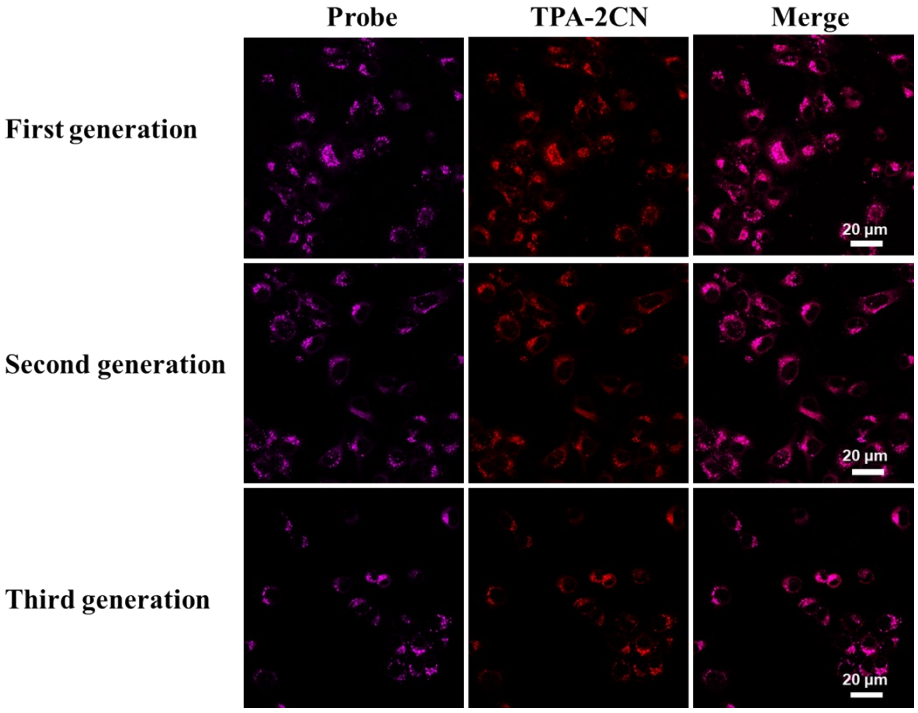

Figure S21. After 1, 2 and 3 generations of cell passage, the CLSM of 4T1 cells was stained using the Golgi-Tracker Red (10 μM) and TPA-2CN (20 μM)

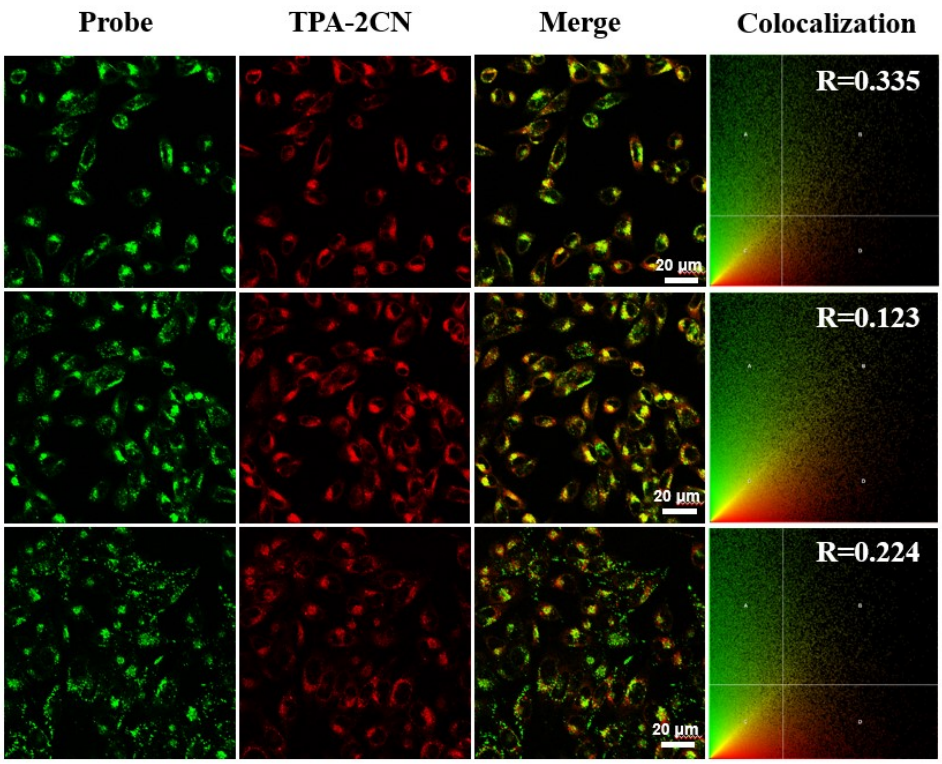

Figure S22. CLSM of 4T1 cells stained with lysosome commercial probes and TPA-2CN.

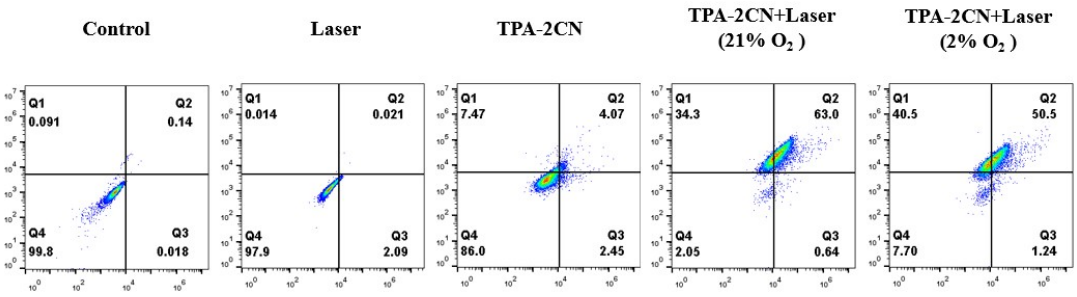

Figure S23. Flow cytometry analysis of 4T1 cells stained with Annexin V-FITC/PI under laser irradiation (0.5 W cm^{-2}, 5 min) with TPA-2CN (20 μM).

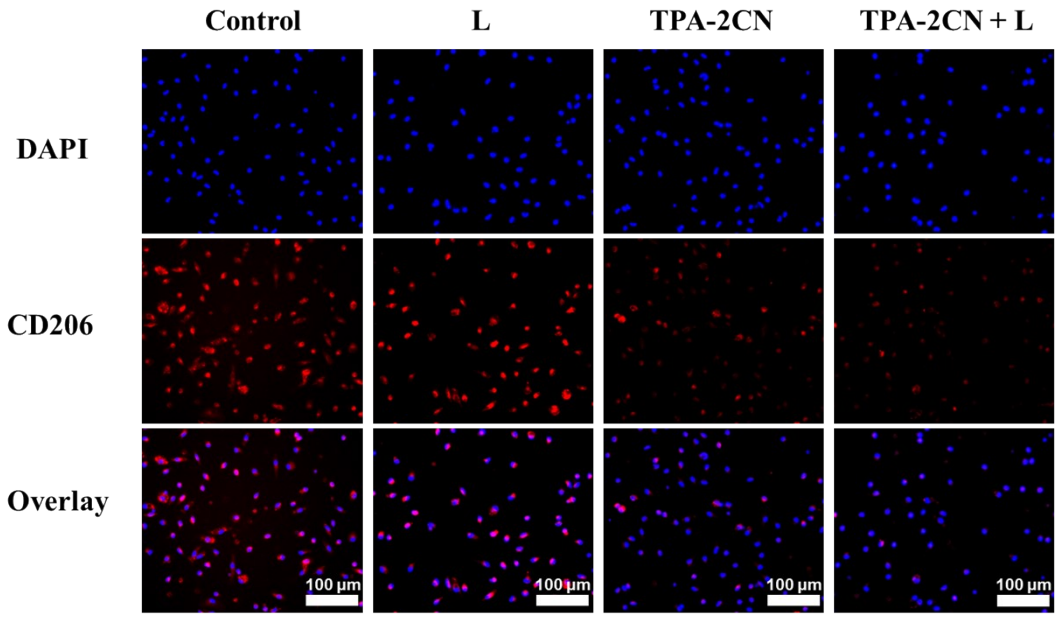

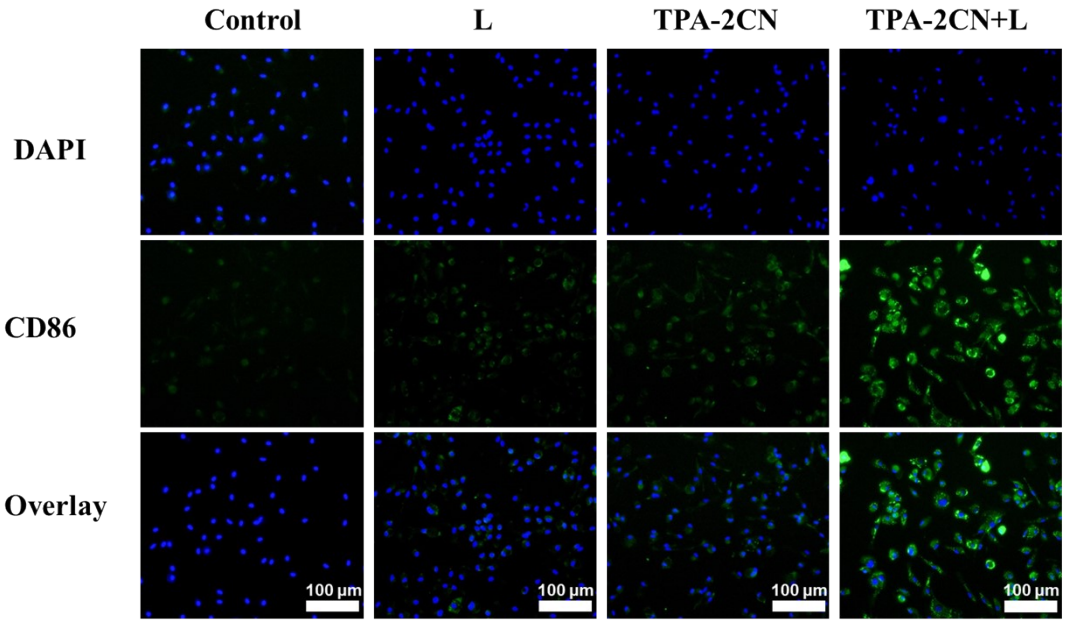

Figure S24. CLSM images of DAPI (nucleus marker), CD206 (M2 marker, red) and CD86 (M1 marker, green) expression after different treatments.

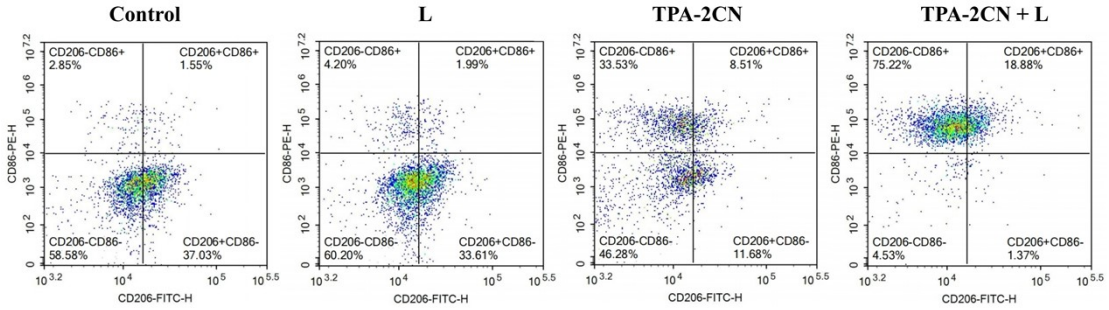

Figure S25. The corresponding quantification of CD206 and CD86 in bone marrow derived macrophages after different treatments.

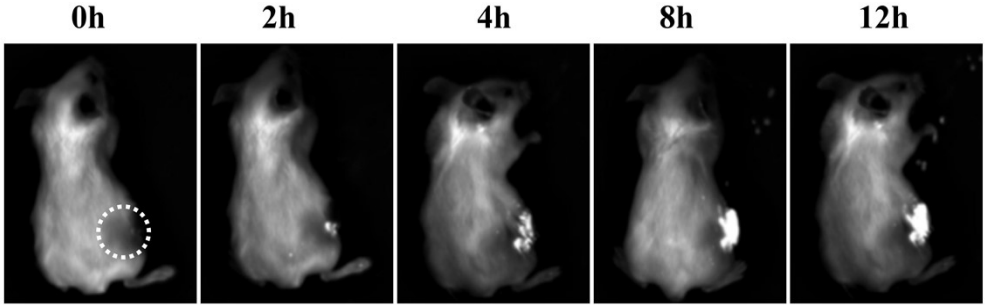

Figure S26. Time-dependent fluorescence imaging of 4T1 tumor mice after injection of TPA-2CN.

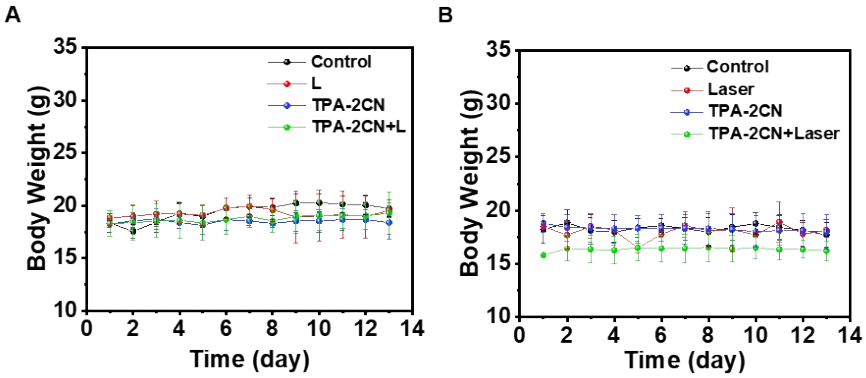

Figure S27. Body weight curves of mice in different treatment groups during treatment under (A) light irradiation (10 mW cm^{-2}) and (B) laser irradiation (0.5 W cm^{-2}), respectively (n = 3). Data are presented as the average ± standard deviation (n = 3); statistical significance: *p < 0.05, **p < 0.01, ***p < 0.001, ****p < 0.0001.

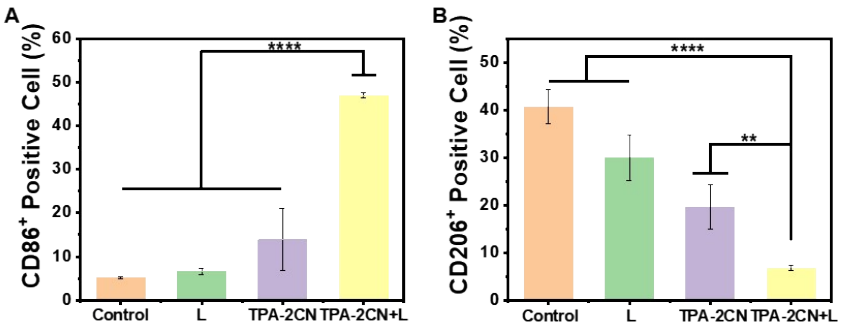

Figure S28. (A) The proportion of the $CD86^+$ in tumor tissues after different treatment (n = 3). (B) The proportion of the $CD206^+$ in tumor tissues after different treatment (n = 3). Data are presented as the average ± standard deviation (n = 3); statistical significance: *p < 0.05, **p < 0.01, ***p < 0.001, ****p < 0.0001.

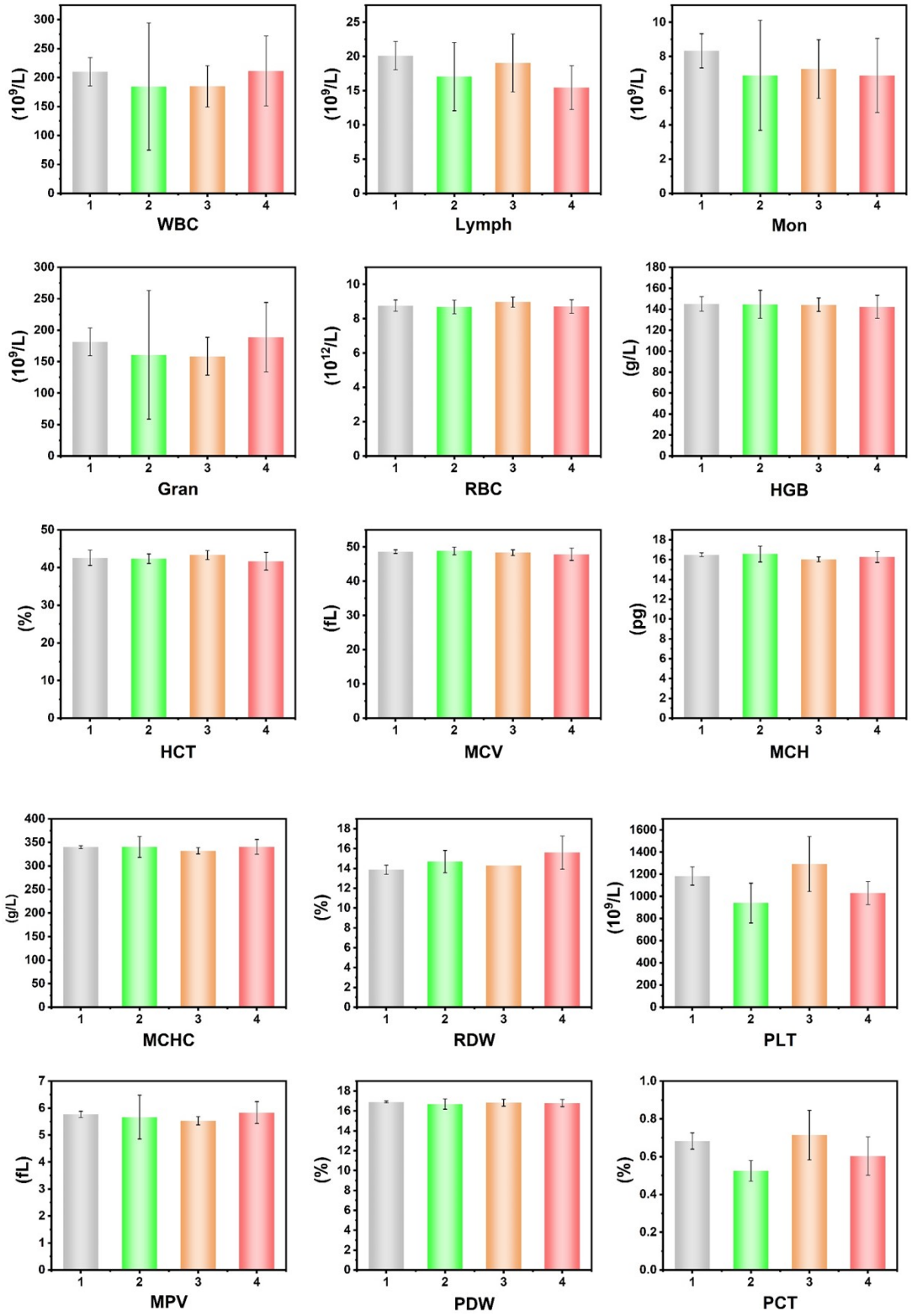

Figure S29. Blood routine indexes of mice after different treatments. The results represent the mean ± standard deviation (n = 3). 1: Control; 2: L; 3: TPA-2CN; 4: TPA-2CN+L.

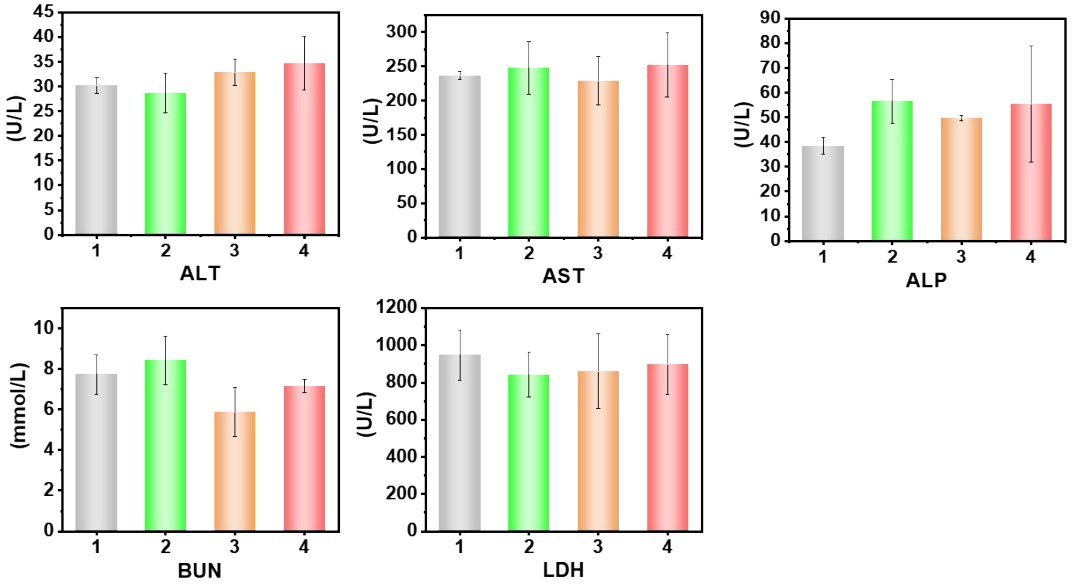

Figure S30. Serum biochemical parameters analyzed with the specimens collected from the animals received various treatments. The levels of blood urea nitrogen (BUN), aspartate alanine aminotransferase (ALT), aminotransferase (AST), lactate dehydrogenase (LDH), and alkaline phosphatase (ALP) were determined by an automated analyzer. The results represent the mean ± standard deviation (n = 3). 1: Control; 2: L; 3: TPA-2CN; 4: TPA-2CN+L.

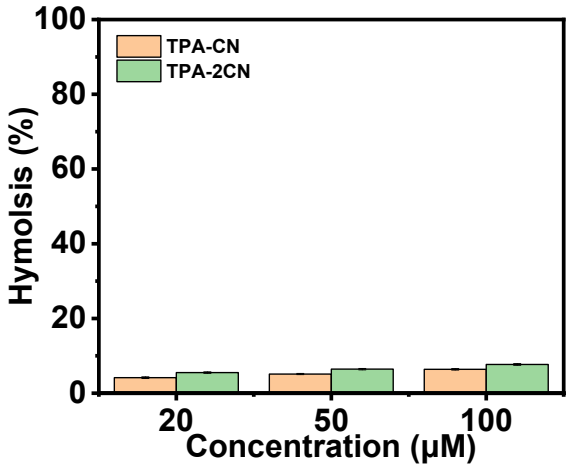

Figure S31. Hemolysis ratio of TPA-CN and TPA-2CN.

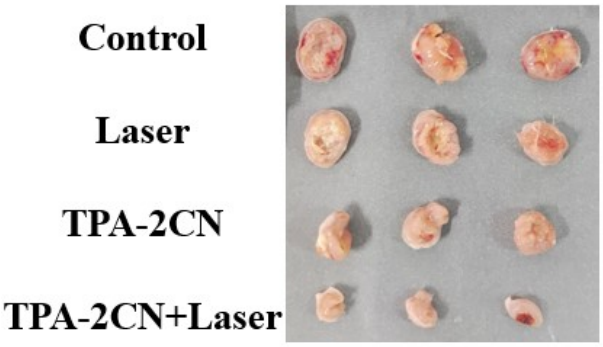

Figure S32. Typical photos of tumors resected from 4T1 tumor-bearing mice at the end of various treatments (n = 3)

References

1. Y. Li, J. Zhuang, Y. Lu, N. Li, M. Gu, J. Xia, N. Zhao and B. Z. Tang, *ACS Nano*, 2021, **15**, 20453-20465.